THE JOURNAL OF BIOLOGICAL CHEMISTRY VOL. 287, NO. 46, pp. 38559–38568, November 9, 2012

Tau Protein Diffuses along the Microtubule Lattice*[S]

Received for publication, April 5, 2012, and in revised form, September 4, 2012 Published, JBC Papers in Press, September 27, 2012, DOI 10.1074/jbc.M112.369785

Maike H. Hinrichs[‡], Avesta Jalal[‡], Bernhard Brenner[‡], Eckhard Mandelkow[§¶], Satish Kumar[§¶], and Tim Scholz[‡1]

From the [‡]Institute for Molecular and Cell Physiology, Hannover Medical School, Carl-Neuberg-Strasse 1, 30625 Hannover, Germany, the [§]German Center for Neurodegenerative Diseases, German Center for Neurodegenerative Diseases, 53175 Bonn, Germany, and the [¶]CAESAR Research Center, Ludwig-Erhard-Allee 2, 53175 Bonn, Germany

Background: Tau protein is believed to be stationary while bound to microtubules.
Results: Tau molecules can diffuse along microtubules over distances up to several micrometers.
Conclusion: Tau diffusion on microtubules is a novel mechanism for Tau dispersion in cells.
Significance: Modulation of Tau binding and diffusion on microtubules by local modifications of microtubules can provide a tool to target Tau to specific cellular compartments.

Current models for the intracellular transport of Tau protein suggest motor protein-dependent co-transport with microtubule fragments and diffusion of Tau in the cytoplasm, whereas Tau is believed to be stationary while bound to microtubules and in equilibrium with free diffusion in the cytosol. Observations that members of the microtubule-dependent kinesin family show Brownian motion along microtubules led us to hypothesize that diffusion along microtubules could also be relevant in the case of Tau. We used single-molecule total internal reflection fluorescence microscopy to probe for diffusion of individual fluorescently labeled Tau molecules along microtubules. This allowed us to avoid the problem that microtubule-dependent diffusion could be masked by excess of labeled Tau in solution that might occur in *in vivo* overexpression experiments. We found that approximately half of the individually detected Tau molecules moved bidirectionally along microtubules over distances up to several micrometers. Diffusion parameters such as diffusion coefficient, interaction time, and scanned microtubule length did not change with Tau concentration. Tau binding and diffusion along the microtubule lattice, however, were sensitive to ionic strength and pH and drastically reduced upon enzymatic removal of the negatively charged C termini of tubulin. We propose one-dimensional Tau diffusion guided by the microtubule lattice as one possible additional mechanism for Tau distribution. By such one-dimensional microtubule lattice diffusion, Tau could be guided to both microtubule ends, *i.e.* the sites where Tau is needed during microtubule polymerization, independently of directed motor-dependent transport. This could be important in conditions where active transport along microtubules might be compromised.

Tau is a structural microtubule-associated protein (MAP)[2] that is located predominantly in the axons of neurons where it supports assembly and stabilization of microtubules (1, 2). In many neurodegenerative diseases Tau protein is highly expressed and mislocated and forms pathological aggregates. It was found that overexpression of Tau in axons inhibits anterograde vesicle and organelle transport (3, 4) and interferes *in vitro* with kinesin and dynein motile functions (5–7). However, despite this interference with microtubule (MT)-dependent and motor-driven transport Tau protein is still able to disperse along axons (3). This led to the proposal of different mechanisms, and their combinations, for physiological distribution of Tau in cells: co-transport with short microtubule fragments along microtubules or actin filaments (8–10), kinesin-driven transport (11, 12), and Tau diffusion in the cytoplasm (10, 13). Yet, in all mechanisms suggested to date, MT-bound Tau is believed to be immobile (in contrast to motor proteins), *e.g.* on a given MT or transported short MT fragment. The immobile Tau, however, is thought to be in equilibrium with freely diffusible Tau in the cytosol (10, 14).

Recently, some members of the MT-dependent kinesin motors family (15–20) as well as the dynein-dynactin complex (21, 22) were shown to exhibit one-dimensional Brownian motion along MTs under conditions in which they are not attached strongly to their MT tracks. Observations that also the kinetochore ring complex Dam-1, the actin-based motor myosin-5, and even charged artificial nanoparticles (23–25) can diffuse along MTs led to the hypothesis that this might be a rather common feature (26). In studies on the kinesin-13 family member MCAK, diffusive motion of single MCAK molecules along MTs was revealed (27), and it was suggested that diffusion along MTs is possible because MCAK is positively charged and partially unstructured. As both features are also true for Tau protein, we hypothesized that diffusive behavior could also be relevant for Tau. One possible additional mechanism for the distribution of Tau could therefore be one-dimensional diffusion guided by the MT lattice. By such one-dimensional MT lattice diffusion (instead of or in addition to directed motor-dependent transport) Tau molecules could reach both ends of the MTs to support MT growth, even in situations when active transport along MTs might be compromised. Additionally, Tau diffusing on a MT could clear the way for passing kinesin or dynein motors under physiological conditions.

* This work was supported in part by Deutsche Forschungsgemeinschaft Research Unit FOR629 grants (to T. S. and E. M.).
[S] This article contains supplemental Figs. S1–S6 and Video 1.
[1] To whom correspondence should be addressed. Tel.: 00495115322094; Fax: 00495115324296; E-mail: scholz.tim@mh-hannover.de.
[2] The abbreviations used are: MAP, microtubule-associated protein; DOL, degree of labeling; MT, microtubule; TIRF, total internal reflection fluorescence; TMR, tetramethyl rhodamine; DTT, dithiothreitol.

We used single-molecule total internal reflection fluorescence (TIRF) microscopy to probe for diffusion of individual fluorescently labeled Tau molecules along immobilized MTs. Diffusion of Tau along MTs has not been observed in cell experiments. In our experiments, the low concentrations of labeled Tau in solution and the TIRF technique allowed to us avoid masking of MT-dependent diffusion of Tau by excess of labeled Tau protein in solution, a problem arising in *in vivo* overexpression experiments. We found that approximately half of the single Tau molecules were able to diffuse bidirectionally along MTs, independently of the Tau concentration and ATP.

EXPERIMENTAL PROCEDURES

Expression and Fluorescence Labeling of Tau Protein—Full-length hTau40 molecules were expressed in *Escherichia coli* as described previously (28). Fluorescent labeling was achieved by incubation of Tau protein reduced by Tris-(2-carboxyethyl)-phosphine with a 7–10-fold molar excess of tetramethyl rhodamine (TMR) or Alexa Fluor 633 maleimide (all Invitrogen), which labeled the two cysteine residues at positions 291 and 322 within the 2nd and 3rd repeat of the assembly domain of hTau40. Unbound fluorescent dye was removed by excessive dialysis against buffer BRB80 (80 mM PIPES, 1 mM $MgCl_2$, 1 mM EGTA, 10 mg/ml glucose, pH 6.8) containing 1 mM dithiothreitol (DTT). The fluorescently labeled Tau protein was then flash frozen and stored at −80 °C until use. Protein concentration, purity, and degree of labeling were tested using SDS-PAGE with subsequent Coomassie stain analysis and using spectroscopic analysis, respectively.

Preparation and Enzymatic Digestion of Microtubules—Paclitaxel-stabilized Cy5- or rhodamine-labeled and unlabeled MTs were prepared basically as described previously (29) except that no biotinylated tubulin was used. Paclitaxel-free Cy5-labeled MTs were digested with 200 μg/ml subtilisin type XXIV (Sigma) for 20 min at 37 °C and stabilized by the addition of Paclitaxel before the digestion was terminated with 2 mM 4-(2-aminoethyl)benzenesulfonyl fluoride hydrochloride (AppliChem). Control samples were incubated under identical conditions but without the proteolytic enzyme. All types of MT were further cleaned by centrifugation through a warm cushion of buffer BRB80 containing 40% glycerol, resuspended in BRB80 with 10 μM Paclitaxel, and stored at room temperature until use.

Single-molecule TIRF Microscopy—A self-made objective type TIRF microscope with single-fluorophore sensitivity (30) was used for the detection of fluorescently labeled MTs and Tau molecules. Prior to immobilization on the surface of the flow chambers (30) the preformed MTs were incubated for 20 min at 35 °C with Tau protein dilutions in buffer BRB12 (12 mM PIPES, 1 mM $MgCl_2$, 1 mM EGTA, 10 mg/ml glucose, pH 6.8) with 10 μM Paclitaxel. During experiments, the assay buffers were supplemented with the desired Tau protein or antibody concentration and 0.5 mg/ml BSA plus 10 μM Paclitaxel and with an oxygen scavenger system (10 mg/ml glucose, 50 units/ml glucose oxidase, 7600 units/ml catalase, and 10 mM DTT) to minimize photodamage of proteins or bleaching of fluorophores. Additionally, 50-μs laser pulses interrupted by 50-μs pauses were used to excite the fluorescently labeled samples. The temperature of 23 °C in the assay chamber was maintained by thermoelectric elements. To test the influence of the ionic strength and pH on the mobility of individual hTau40-TMR molecules assay buffers of different pH values were used or additionally supplemented with different concentrations of potassium acetate. Movement of fluorescently labeled Tau molecules with a degree of labeling (DOL) of 200% (*i.e.* complete labeling of the two cysteines) or antibody molecules was recorded for time periods of 60 s with 5 frames/s.

Data Analysis—Data were recorded and converted to tif stacks using the camera program Andor Solis (Andor Technology, Belfast, Ireland). Individual fluorescently labeled molecules were located and tracked using the computer program ImageJ (National Institutes of Health) and the plug-ins *Multiple Kymograph* (J. Rietdorf and A. Seitz, EMBL, Heidelberg, Germany) and *Particle Tracker* (31). The validity of each trajectory was confirmed by visual inspection. Particles that remained stationary, switched between clear stationary and mobile periods, repetitively reached one end of a MT, and overlapping trajectories of adjacent molecules were excluded from analysis. Mean squared displacements, scanned MT distances, and interaction times of tracked particles were calculated using Microsoft Excel 2003, and the data were fitted with Origin 7 (OriginLab, Northampton, MA).

RESULTS

Tau Protein Is Not Stationary on Microtubules, and Its Mobility Can Be Described as Diffusion along the Microtubule Lattice—In the published models for the dispersion of Tau protein in cells, Tau is believed to be stationary when bound to a given MT but in equilibrium between MT-bound and diffusing freely in the cytosol. To test for one-dimensional Tau diffusion guided by the MT lattice we used single-molecule TIRF microscopy to visualize individual Tau molecules on immobilized MTs. Single tetramethyl rhodamine-labeled Tau molecules (hTau40-TMR) co-localized with immobilized Cy5-labeled MTs (Fig. 1*A*). However, approximately 50% of the Tau molecules were not stationary on the MTs but exhibited undirected motion along the immobilized MTs for periods of several seconds and over distances of several micrometers (Fig. 1, *B* and *C*). In addition to using highly purified proteins (supplemental Fig. S1), we performed these experiments also in the absence of ATP to rule out the possibility that this motion might be a result of motor protein action. The mobility of Tau molecules along MTs could be described by one-dimensional diffusion because plots of the mean squared displacements $<x^2>$ of mobile hTau40-TMR molecules against the time increment (Fig. 1*D*, *black squares*) could be fitted by linear regressions (Fig. 1*D*). The diffusion coefficient D was derived from the slope of this regression, which follow the equation $<x^2> = 2Dt$. In contrast, single kinesin molecules moving uni-directionally along MTs while consuming ATP generated parabolic plots of their mean squared displacement against the time increment (Fig. 1*D*, *gray circles*). To test for such an additional directional bias in our data of single mobile Tau molecules, polynomial fits to the equation $<x^2> = 2Dt + (vt)^2$ for diffusion plus directed motion were performed. As in the example shown in Fig. 1*D*, no evidence for directed velocity v was found, and the apparent

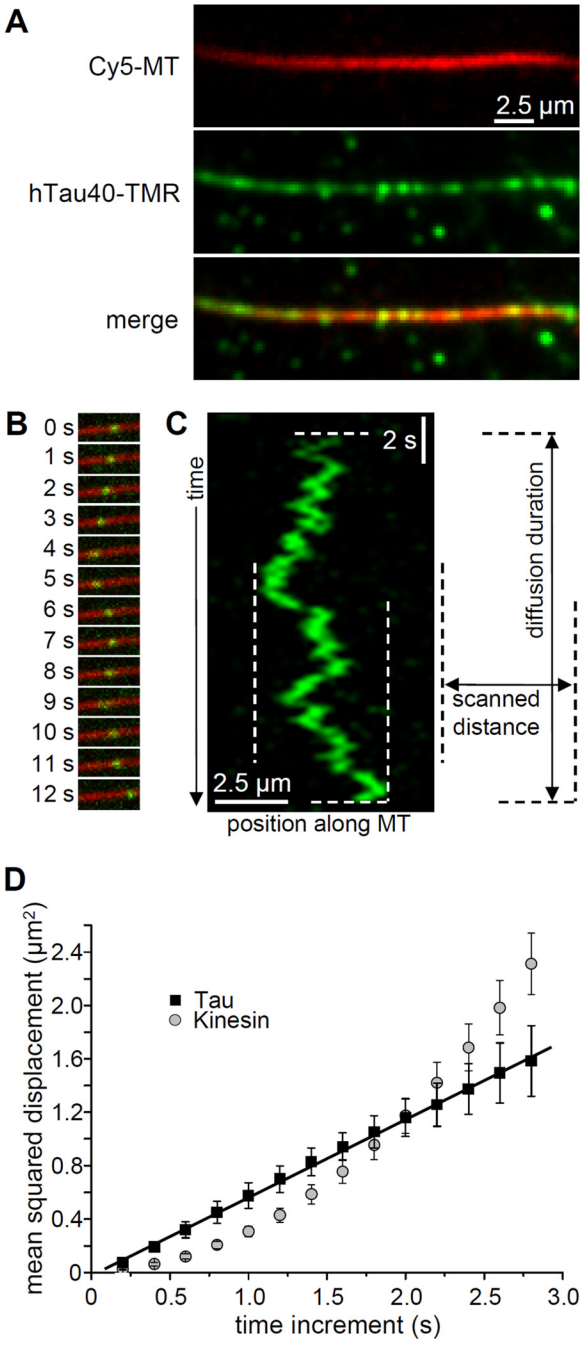

FIGURE 1. **Tau molecules diffuse along MTs.** *A*, TIRF microscopy images of a Cy5-labeled MT (*red*) and TMR-labeled hTau40 molecules (*green*) at a Tau:tubulin ratio of 100 pM:50 nM. hTau40-TMR shows clear co-localization and enrichment on Cy5-labeled MTs. *B*, sequential frames of a TMR-labeled hTau40 molecule (*green*) moving along an immobilized Cy5-labeled MT (*red*) in the absence of ATP. The Tau:tubulin ratio was 100 pM:50 nM. Only 5% of the Tau molecules were TMR-labeled. Time intervals were as indicated. *C*, kymograph of the movement of the hTau40-TMR molecule shown in *B*. *Horizontal dashed lines* indicate start and end of diffusive interaction, respectively. The extreme positions along the MT reached during this diffusive encounter of ~15 s are depicted as *vertical dashed lines*. *D*, mean squared displacement $<x^2>$ of the same hTau40-TMR molecule (*black squares*) plotted against time increment, *i.e.* different time intervals over which displacement was determined. Data fitted by a linear regression (*black line*) to the equation $<x^2> = 2Dt$ yielded a diffusion coefficient D of 0.292 $\mu m^2/s$. As an example for directed motion the *gray circles* depict data derived from a single kinesin-1 molecule moving linearly along an MT with a speed of 0.481 $\mu m/s$ in the presence of 1 mM ATP. *Error bars* represent the S.E. of the squared displacement values.

velocities of the tracked Tau molecules had a Gaussian distribution around zero (-0.012 ± 0.010 $\mu m/s$). Therefore, we conclude that movement of Tau along MTs did not include any uni-directional component.

The undirected diffusive motion of Tau on MTs was neither caused nor significantly affected by the fluorophores/fluorescent labels. The tetramethyl rhodamine dye alone did not show mobility along MTs, and the observed diffusion of Tau molecules was not dependent on Tau or MT labeling in different combinations (Fig. 1 and supplemental Fig. S2, *A* and *B*; see Fig. 4*B*), and the derived diffusion coefficients were almost identical (hTau40-TMR (200% DOL) on Cy5-labeled MTs: $D = 0.153 \pm 0.019$ $\mu m^2/s$, $n = 170$; hTau40-TMR (10% DOL) on Cy5-labeled MTs: $D = 0.142 \pm 0.026$ $\mu m^2/s$, $n = 20$; hTau40-TMR on unlabeled MTs: $D = 0.169 \pm 0.029$ $\mu m^2/s$, $n = 13$; hTau40-Alexa633 on rhodamine-labeled MTs: $D = 0.164 \pm 0.013$ $\mu m^2/s$, $n = 9$). To test whether the observed diffusion of Tau molecules might be the result of labeling the intrinsic cysteine residues within the second and third repeats of the assembly domain we made use of a Tau construct that was labeled at a different site. In this construct (cys-lite hTau40*I260C*-Alexa488) both cysteine residues in R2 and R3 were changed to alanine and a new cysteine was introduced at position 260 and labeled with Alexa Fluor 488 maleimide. We found that this construct diffused robustly along MTs (supplemental Fig. S2*C*).

The Diffusive Behavior of Tau Is Independent of Its Concentration—We characterized the diffusive behavior of individual Tau molecules (supplemental Fig. S3) in a wide concentration range between subphysiological 2 pM and elevated 10 nM Tau at constant 50 nM MTs. At hTau40-TMR concentrations exceeding 20 pM, trajectories of individual molecules could no longer be discriminated, and higher total concentrations of Tau protein were achieved by mixing 5–10 pM labeled with unlabeled hTau40. Surprisingly, the diffusion coefficient, the diffusion duration, and also the MT distance scanned by diffusing individual Tau molecules did not change with increasing total Tau concentration on the MTs (Fig. 2, *A*, *C*, and *E*). We tracked 170 individual hTau40-TMR molecules and calculated their average diffusion coefficient D to be 0.153 ± 0.019 $\mu m^2/s$ (Fig. 2*B*). The durations of diffusive interactions distributed exponentially (Fig. 2*D*) and yielded a mean lifetime t of 24.41 ± 1.78 s when corrected for photobleaching (supplemental Fig. S5*D*). We calculated the average microtubule length scanned by single diffusing Tau molecules (scanned distance) from the average diffusion coefficient and diffusion duration (27) to be 2.73 ± 0.14 μm ($\sqrt{2Dt}$), which agrees well with the main peak in the measured data (Fig. 2, *E* and *F*). Note that the values plotted in Fig. 2*F* contain both an increasing component derived from the root mean spare displacement and a decreasing component from the exponential decay of the interaction time (Fig. 2*D*). Within the tested range between 2 pM and 10 nM the fraction of mobile Tau molecules did not change with increasing total Tau concentration but remained at ~50% (supplemental Fig. S4). Additionally, we performed experiments using single-labeled hTau40-TMR molecules with a DOL of only 10%. The values for single-labeled hTau40-TMR molecules (supplemental Fig. S5, *A–C*, $D = 0.142 \pm 0.026$ $\mu m^2/s$; $t = 22.81 \pm 2.85$ s; scanned distance $= 2.545 \pm 0.222$ μm) were very

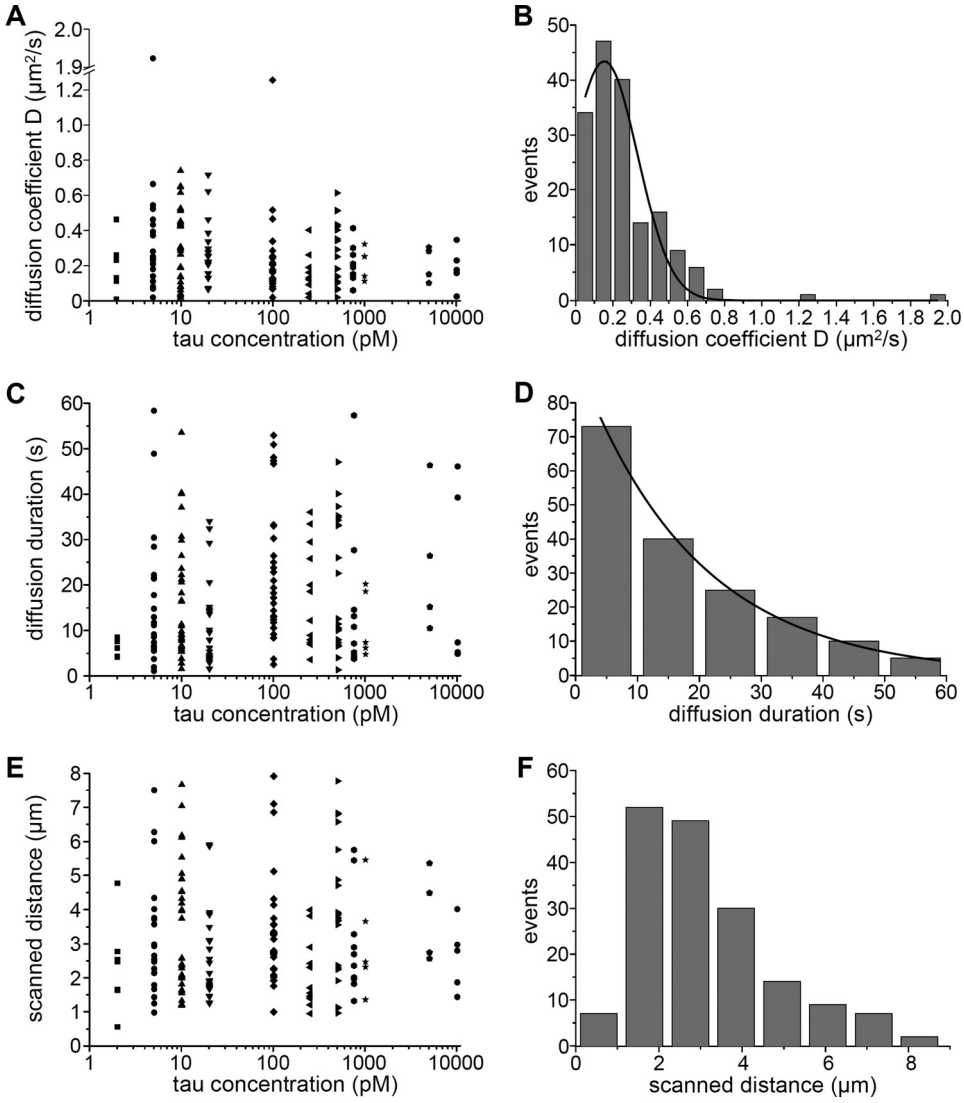

FIGURE 2. **The diffusive behavior of Tau molecules is independent of the total Tau concentration.** *A*, diffusion coefficients of individual hTau40-TMR molecules at different Tau concentrations. Concentration of tubulin was 50 nM. *B*, distribution of diffusion coefficients of 170 hTau40-TMR molecules at various total Tau concentrations. A Gaussian fit (*black curve*) yielded a mean value for the diffusion coefficient *D* of 0.153 ± 0.019 $\mu m^2/s$. *C*, interaction times between individual hTau40-TMR molecules and Cy5-labeled MTs at different Tau concentrations in the presence of 50 nM tubulin. *D*, distribution of interaction durations of 170 hTau40-TMR molecules at various total Tau concentrations. An exponential decay (*black curve*) fitted to the data yielded, when corrected for photobleaching (supplemental Fig. S5*D*), a diffusion time constant of 24.41 ± 1.78 s. *E*, distances on MTs scanned by individual hTau40-TMR molecules during their interaction times at different Tau concentrations in the presence of 50 nM tubulin. *F*, distribution of observed distances on MTs scanned by individual hTau40-TMR molecules ($n = 170$) at various total Tau concentrations.

comparable with the values gained from double-labeled hTau40-TMR, again indicating that the DOL did not effect the diffusive behavior of Tau molecules.

Occasionally, we observed transitions from stationary to mobile periods (or vice versa) of individual Tau molecules (supplemental Fig. S6). As these events were rather rare and occurred with rates of ~0.015 s^{-1} (18 and 20 transitions, respectively, in totally 1287 counted mobile and stationary Tau molecules each recorded for 60 s), we conclude that for individual Tau molecules transitions from a stationary to a mobile state or vice versa are possible, but the lifetimes of these states are long and usually exceed our observation period of 60 s.

Tau Uses the C Terminus of Tubulin as an Interaction Partner for Diffusion along the Microtubule Lattice—It has been shown that some MT-binding proteins use the C-terminal peptide of tubulin, the so-called E-hook, for diffusion along the MT lattice (20, 27) whereas others do not (15, 32). After enzymatic removal of the tubulin C terminus by subtilisin (Fig. 3*C*) the number of MT-bound Tau molecules decreased substantially (by ~70%) (Fig. 3*A*), and most of them remained stationary bound on these Cy5-labeled MTs (Fig. 3*B*, *kymographs 1–3*). Only very few diffusible molecules were detected which showed brief and slow movement (Fig. 3*B*, *rightmost track* in *kymograph 3*). However, at the same time in the very same assay chambers bidirectional motion of hTau40-TMR molecules along unlabeled undigested MTs was observed (Fig. 3*B*, *kymographs* † and ‡). The diffusion coefficient of hTau40-TMR on unlabeled undigested MTs in these "mixed MT" diffusion assays with an average value of 0.169 ± 0.029 $\mu m^2/s$ ($n = 13$) was found to be identical to values derived from hTau40-TMR molecules diffusing along Cy5-labeled MTs (Fig. 2*B*).

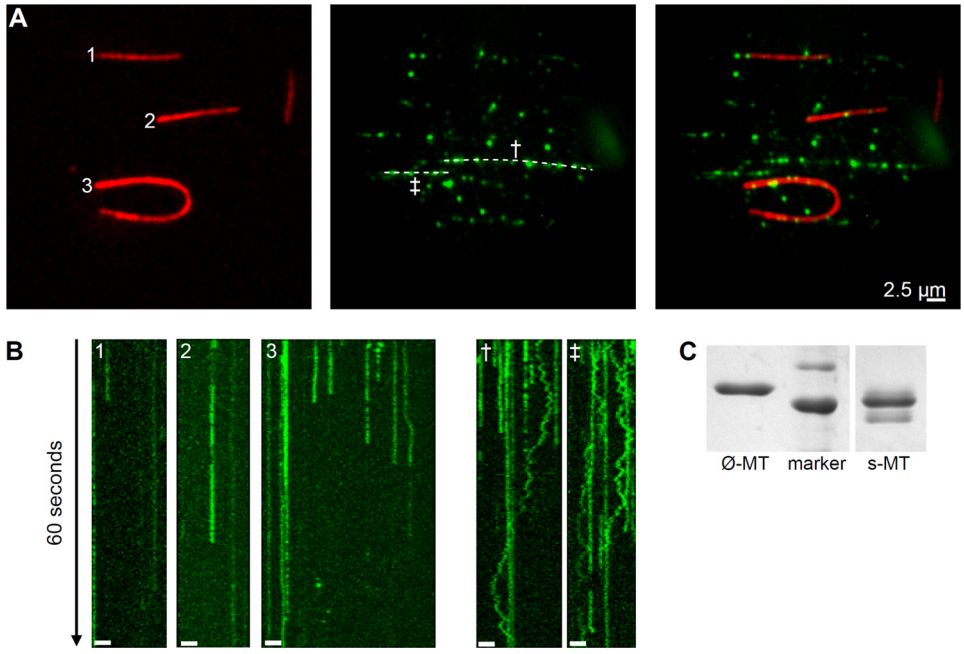

FIGURE 3. **The C terminus of tubulin facilitates Tau binding to MTs and Tau diffusion.** *A*, TIRF microscopy images of three (*1–3*) Cy5-labeled subtilisin-digested MTs (*red*) immobilized together with unlabeled undigested MTs. TMR-labeled hTau40 molecules (*green*) bound preferentially to undigested but not to subtilisin-digested MTs, making the unlabeled undigested MTs visible (indicated as *dashed white lines*). *B*, 60-s kymographs of few but mainly stationary hTau40-TMR molecules on Cy5-labeled subtilisin-digested MTs (*1–3*, from *A*). More hTau40-TMR molecules bound to two unlabeled undigested MTs († and ‡, from *A*) and showed clear movement. *Scale bars*, 2.5 μm. *C*, Coomassie Brilliant Blue-stained SDS-PAGE of undigested unlabeled MTs (*Ø-MT*) and partially Cy5-labeled subtilisin-digested MTs (*s-MT*, 200 μg/ml subtilisin for 20 min at 35 °C), marker: 50, 60 kDa.

Tau Binding and Diffusion along Microtubules Are Sensitive to Ionic Strength and pH—As the negatively charged C terminus of tubulin facilitated diffusive motion of Tau molecules along MTs, we tested whether the observed diffusion of individual Tau molecules along MTs is mediated by electrostatic interactions and is therefore sensitive to ionic strength or pH. Hence, we supplemented potassium acetate in our assays to mimic the *in vivo* ionic environment (33, 34) and performed our single-molecule diffusion assays in buffers of increasing ionic strength (from ~40 mM in buffer BRB12 with no potassium acetate added to 140 mM in BRB12 with additional 100 mM potassium acetate). We found that the diffusion coefficient of hTau40-TMR molecules increased with increasing ionic strength (Fig. 4*A* and Table 1). At the same time the number of Tau molecules and the durations of the diffusive interactions with MTs decreased with increasing ionic strength (Fig. 4*B* and Table 1). As a result, the MT segment ($\sqrt{2Dt}$) scanned by an hTau40-TMR molecule during such a diffusive interaction remained unchanged (Fig. 4*C* and Table 1). Unlike the diffusion coefficients and durations, however, the fraction of mobile Tau molecules did not change with increasing ionic strength but remained at 50–54% (Table 1). The diffusive parameters of Tau molecules were also highly dependent on the pH of the experimental solution. Whereas the fraction of mobile Tau molecules between pH 6.0 and 8.0 remained unchanged at 46–54% (Table 1) the increase in the diffusion coefficient with increasing pH was even more pronounced than with increasing ionic strength (Fig. 4*D* and Table 1). The durations of the diffusive interactions decreased at higher pH, leaving the MT distance scanned by individual Tau molecules almost constant (Fig. 4, *E* and *F*, and Table 1). At pH 6.0 only very few Tau molecules could be observed to bind to and diffuse slowly along MTs.

Diffusion along Microtubules May Be a General Feature Even for Non-MAPs Such as Antibodies—Recently it has been reported that even artificial charged nanoparticles can diffuse along MTs, suggesting that one-dimensional Brownian motion along rod-like polymers is electrostatic in origin rather than depending on specific tertiary structures (24). To test whether diffusive movement along MTs is a rather general feature we tested other proteins that were not known to bind to MTs. Because Fc fragments of antibodies are overall positively charged we tested the monoclonal IgG antibody m74-1 which is specific for the intermediate chain of dynein (35) for its ability to diffuse along the MT lattice. We labeled the immunoglobulin with rhodamine using a rhodamine antibody labeling kit (Thermo Scientific) and found that the labeled antibody exhibited one-dimensional diffusion along MTs (Fig. 5*A*), yet with a lower diffusion coefficient (Fig. 5*B*) compared with Tau molecules or the kinesin family member MCAK (27). 74.81 ± 5.62% (S.D.) of the observed antibodies exhibited one-dimensional diffusion whereas ~25% remained stationary. The example shown in Fig. 5*B* yielded a diffusion coefficient D of 0.0497 $\mu m^2/s$. The average diffusion coefficient D was found to be 0.0602 ± 0.0172 $\mu m^2/s$ (S.E., $n = 11$), and the majority (8 of 11; 73%) of polynomial fits to the equation $<x^2> = 2Dt + (vt)^2$ gave negative values for directed velocity, in this example v = 0.0654 μm/s. Therefore, movement of antibodies along MTs was found to be diffusive and had no component of directional bias.

DISCUSSION

In neurons, Tau needs to be transported and sorted into different cellular compartments. Current models for the dispersion of Tau protein involve co-transport of bound Tau with

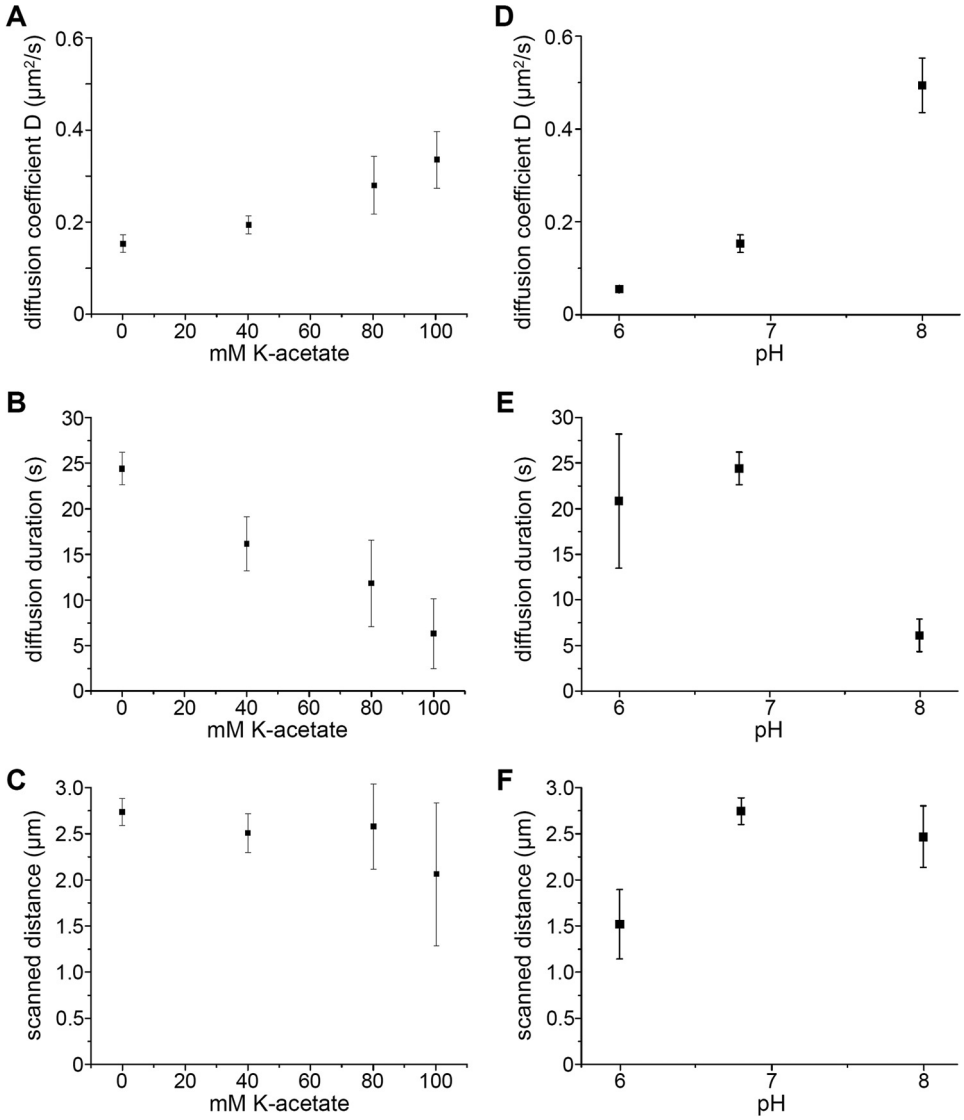

FIGURE 4. **The diffusion of Tau molecules along MTs is sensitive to ionic strength and pH.** *A*, diffusion coefficient *D* of TMR-labeled hTau40 molecules diffusing along MTs *versus* potassium acetate concentration added to buffer BRB12 resulting in final ionic strength of ~40, 80, 120, and 140 mM, respectively. *Error bars* represent error margins of the Gaussian fits. *B*, diffusion time, corrected for photobleaching, of TMR-labeled hTau40 molecules *versus* potassium acetate added to buffer BRB12. *Error bars* represent error margins of the exponential decay fits to the observed duration and the TMR fluorescence decay. *C*, MT sections scanned by hTau40-TMR molecules (calculated from the diffusions constants and the respective corrected interaction times) *versus* potassium acetate concentration. Error margins were calculated from the error margins in *A* and *B*. *D*, diffusion coefficient *D* of hTau40-TMR molecules diffusing along MTs *versus* pH of buffer BRB12. *Error bars* represent error margins of the Gaussian fits. *E*, photobleaching corrected diffusion time of hTau40-TMR molecules *versus* pH of buffer BRB12. *Error bars* represent error margins of the exponential decay fits to the observed duration and the TMR fluorescence decay. *F*, MT sections scanned by hTau40-TMR molecules *versus* pH of buffer BRB12 (calculated from the respective diffusions constants and interaction times). Error margins were calculated from the error margins in *E* and *F*.

short MT fragments (8–10), kinesin-driven transport (11, 12), and Tau diffusion in the cytoplasm (10, 13). Consequently, so far MT-bound Tau is believed to be stationary on a given MT or transported MT fragment but in equilibrium with diffusible Tau in the cytosol (10, 14). Using single-molecule TIRF microscopy, we found that about half of the individually detected Tau molecules on MTs were not stationary but moved bidirectionally along these MTs.

In contrast to the reported kinesin-driven transport of Tau protein (11, 12), the observed diffusion of individual Tau molecules along MTs was independent of motor proteins as highly purified proteins were used and Tau diffusion along MTs occurred in the absence of ATP. Additionally, no indication of a directional bias was found, which would be expected if this mobility was motor-driven. Therefore, the observed mobile behavior most likely is an intrinsic property of Tau and due to a direct interaction of Tau and MTs. However, our data do not exclude an additional long range kinesin-driven transport of Tau in cells.

Is the observed mobility the diffusion of individual Tau molecules? In addition to one- and two-step photobleaching of double-labeled hTau40-TMR molecules (Fig. S3, *A* and *B*), we analyzed the fluorescence intensities of diffusing Tau molecules and of Tau molecules stationary bound on MTs (Fig. S3*C*), which revealed several important points: (i) Stationary spots were not higher in fluorescence intensity than diffusing molecules, arguing against the idea that stationary spots were composed of aggregates of diffusible Tau molecules. (ii) The diffus-

TABLE 1

Tau binding and diffusion along microtubules is sensitive to ionic strength and pH

Diffusion parameters, corrected for photobleaching, of single hTau40-TMR molecules in buffers of increasing ionic strength (buffer BRB12 with ~40 mM ionic strength supplemented with various concentrations of potassium acetate) or different pH. Errors reported for diffusion coefficients, diffusion durations, and scanned distances are given as error margins of Gaussian fits, error margins of exponential decay fits, and error margins calculated from the latter two, respectively. The calculations of the fraction of mobile Tau molecules at different ionic strength account not only for analyzed mobile Tau molecules (tracked molecules) but also for immobile Tau molecules and mobile molecules that were excluded from analysis due to limitations mentioned in the experimental procedures. To account for slight variability between different experiments under the same experimental conditions, average values ± S.D. of independent experiments are given.

Buffer BRB12						
pH	Potassium acetate added	Diffusion coefficient	Tracked molecules	Diffusion duration	Scanned distance	Mobile Tau molecules
	mM	$\mu m^2/s$		s	μm	%
6.8	0	0.153 ± 0.019	170	24.41 ± 1.78	2.733 ± 0.144	53.5 ± 1.1
6.8	40	0.194 ± 0.019	40	16.18 ± 2.95	2.506 ± 0.207	49.7 ± 1.3
6.8	80	0.280 ± 0.063	21	11.84 ± 4.76	2.575 ± 0.461	54.0 ± 2.2
6.8	100	0.336 ± 0.062	12	6.31 ± 4.74	2.059 ± 0.774	51.8 ± 3.1
6.0	0	0.055 ± 0.007	13	20.84 ± 7.36	1.514 ± 0.375	46.2 ± 2.3
8.0	0	0.494 ± 0.059	25	6.11 ± 2.70	2.457 ± 0.458	52.6 ± 9.4

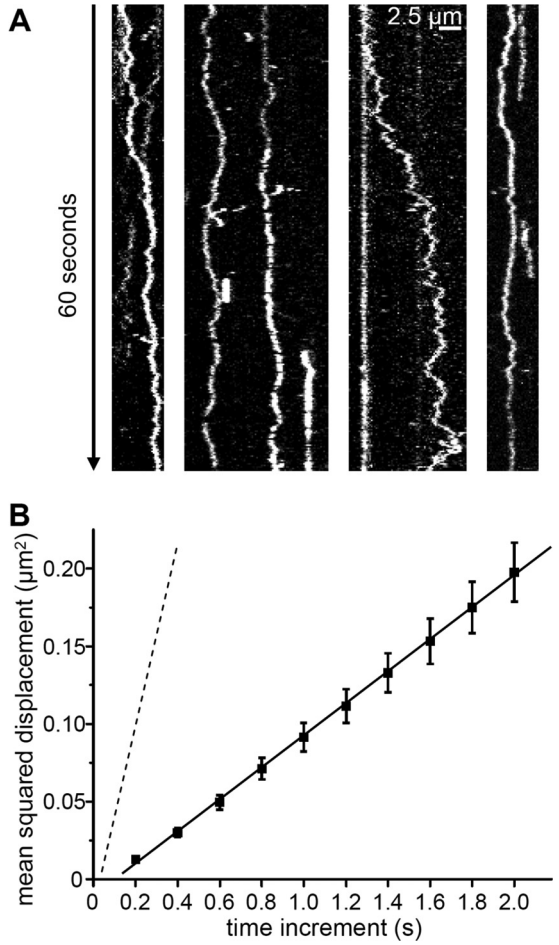

FIGURE 5. **Diffusion of an IgG antibody along immobilized MTs.** *A*, 60-s kymographs of rhodamine-labeled anti-dynein IgG antibodies (40 ng/ml) moving bidirectionally along two different immobilized Cy5-labeled MTs. *B*, mean squared displacement $<x^2>$ (*black squares*) of a rhodamine-labeled antibody (bright mobile molecule in the *leftmost kymograph* in *A*) plotted against the time increment. The data were fitted by a linear regression (*black line*) to the equation $<x^2> = 2Dt$ yielding the diffusion coefficient D (0.0497 $\mu m^2/s$). *Error bars* represent the S.E. of the squared displacement values. For comparison, the *dashed line* represents data derived from the diffusing hTau40-TMR molecule shown in Fig. 1*D*.

ing spots showed a bimodal distribution in the same range of fluorescence intensity values as found for the stationary ones. (iii) Tau molecules, which underwent two-step photobleaching during diffusion, dropped in their fluorescence intensity to ~50% of their initial intensity and not more as would be expected for larger aggregates. Additionally, a decrease of fluorescence intensity in more than two steps, *i.e.* 100%, ~50%, off or detachment, was not observed. These findings suggest that the bimodal distribution represents double- and single-(already bleached once) labeled Tau molecules and that the stationary fluorescent spots on MTs, too, represent single Tau molecules and not aggregates.

The properties of diffusing Tau molecules did not change with increasing total Tau concentrations. Due to possible Tau clustering on the MTs, one might have expected that with increasing total Tau concentration the dwell times of Tau might increase whereas the diffusion coefficient and the scanned MT distance would decrease. This was not observed in our experiments, which suggests that the published inhibitory effect of Tau on motor proteins cannot be explained by pure sterical blocking. Diffusing Tau molecules could give way to passing kinesin or dynein motors (as postulated in Ref. 26) as individual Tau molecules were still mobile on MTs even at Tau levels where kinesin inhibition has been observed.

In axons, a diffusion coefficient for hTau40 of ~3 $\mu m^2/s$ and an average MT interaction time of ~4 s have been found and were interpreted as an almost free diffusion of Tau in the cytosol interrupted by brief periods of stationary binding to MTs (10). Yet, it has been observed before that one-dimensional diffusion tends to be significantly slower than motion in three dimensions (23, 27, 36). At physiological ionic strength, we found dwell times for Tau on MTs (~6 s) comparable with previous reports. During these transient interactions, however, Tau molecules could diffuse one-dimensionally along MTs with diffusion coefficients of up to 0.34 $\mu m^2/s$, thus scanning ~2.7 μm of MT length. Our results do not contradict previous findings but open a new window on the understanding of Tau dispersion in cells, namely an additional mechanism for Tau dispersion by one-dimensional diffusion along the MT lattice.

Already at the lowest ionic strength used in our experiments single Tau molecules diffused along MTs as suggested by the brightness analysis of diffusing and static Tau molecules (supplemental Fig. S3*C*). The observed increase of the diffusion coefficient of Tau molecules with increasing ionic strength is therefore unlikely to be due to changes in the oligomerization state of Tau molecules. Such an increase of the diffusion coefficient with ionic strength is also consistent with previous

reports, *e.g.* on the Ndc80 kinetochore complex (37) and on full-length kinesin-5 molecules diffusing tail-dependently along MTs (38). In the latter study, addition of 40 mM potassium chloride led to an almost 3-fold increase in the diffusion coefficient of individual kinesin-5 molecules. In our experiments, an even greater increase in the diffusion coefficient was found for Tau molecules diffusing along MTs at different pH (Fig. 4, *D–F*). Here, one could think of possibilities other than pure electrostatic reasons: the repeat domain of Tau contains some (transient) secondary structure elements such as β-strands and turns, which might undergo some conformational changes (39, 40). Additionally, Tau has a preferred "paperclip" conformation in solution (41, 42), and it is possible that this conformation is perturbed in the presence of tubulin as a function of pH.

Is Tau diffusion restricted to just one protofilament, or is Tau able to switch between protofilaments during a diffusive encounter with a MT? To test for protofilament switching or to resolve possible Tau hopping between adjacent tubulin E-hooks during diffusion along MTs, a spatial resolution of 4 nm or better is needed at the frame rates necessary for characterization of Tau diffusion. Such a high resolution could not be achieved in our experiments, and therefore switching of diffusing Tau molecules between protofilaments could not be observed directly. Nevertheless, we recall that the diffusion coefficient of Tau does not decrease with increasing Tau concentration on MTs, the duration of diffusive interactions does not get shorter, and the MT length scanned during a diffusive interaction does not change. All of this suggests that Tau molecules diffusing along the length of a MT do not block but rather pass each other, either because they are bound to neighboring protofilaments or by switching onto another protofilament. In addition, we occasionally observed switching between intersecting MTs (supplemental Video 1), which could mean that Tau can easily change between protofilaments, even of different MTs, without detaching or with detached periods too brief to be detected. We therefore conclude that Tau molecules are able to change from one to another protofilament when diffusing along a MT.

From structural and biochemical approaches it has been concluded that Tau might have more than one binding conformation or binding site on MTs (43–46). Such different binding modes could result in different populations of Tau molecules on MTs with distinct properties and functions. However, the structural and functional consequences of these different Tau binding modes have not been studied, although a certain mobility of Tau molecules on MTs has been proposed (45). In our experiments, almost 75% of anti-dynein antibodies were mobile along MTs, which is more than ~50% mobile molecules found in the case of hTau40-TMR but significantly less than 100%. This led us to conclude that these 25% immobile antibodies, as well as part of the immobile population of Tau molecules, might possibly be due to molecules stuck to the coverslip surface near MTs or due to molecules trapped by defects in the MT lattice as suggested for MCAK molecules diffusing along MTs (27). Such lattice defects are known to occur in *in vitro* assembled MT (47). Recently, the actin-based motor myosin-5, which can additionally bind and diffuse along MTs, was reported to occupy two different binding states on MTs: one diffusive and one immobile "trapped" state (32). It was concluded that the immobile trapped state was achieved if, in addition to electrostatic interactions, also non-ionic attraction forces became dominant. Our observation of an immobile and a diffusive population of Tau molecules on MTs might be explained in a comparable fashion. Alternatively, a combination of different Tau conformations and the interaction of different Tau domains with the MT lattice could also lead to distinct mobile properties of Tau molecules. At least parts of these two populations are interchangeable as Tau molecules can switch between the mobile and trapped state, although only slowly.

Here, we report that the MAP Tau can diffuse one-dimensionally along the MT lattice, but is this feature exclusive to MAPs and molecular motors? It was observed previously that MTs can diffuse along their axis on glass surfaces coated with methylcellulose (48); and recently, charged artificial nanoparticles were reported to diffuse along MTs (24). Our finding that even a randomly selected antibody diffused along MTs supports the idea that one-dimensional diffusion along the microtubule lattice might be a rather common means of dispersion in cells. For such a diffusing molecule, attractive and repulsive charge-charge interactions between the diffusing molecule and the MT need to be well balanced to prevent premature detachment from or immobilization on MTs (24, 32). In cells, this balance could be modulated locally to create patterning or asymmetric distributions of proteins (49–51). In the case of MTs and Tau, this could be achieved by local modifications of MTs or Tau modifications. Phosphorylation of Tau (*e.g.* by the kinase MARK/Par-1) detaches Tau from MTs in cells and decreases the dwell time of their interaction. Tau diffusion along the microtubule lattice was found to be sensitive to the presence of the negatively charged C terminus of tubulin (E-hook). Therefore, one tool to differentially recruit MAPs to distinct regions of a neuron such as dendrites or the axon might also be different nucleotide states of MTs (52, 53) or post-translational modifications of tubulin as proposed for kinesin-1 (54).

In summary, we could show that Tau, in addition to reported free diffusion in the cytosol and binding to MTs, can also diffuse one-dimensionally along MTs. Advantages of such diffusion guided by the MT lattice would be that (i) no external chemical energy is needed, (ii) both ends of the MT can be targeted, (iii) Brownian motion is faster than active transport over short distances of up to 1 μm, and (iv) a more even distribution on MTs can be achieved due to frequent transitions between protofilaments. Modulation of Tau binding and diffusion on MTs by local post-translational modifications of MTs or Tau can also provide a tool to target Tau into axons or to missort Tau into dendrites upon failure during neurodegeneration.

Acknowledgments—We thank Ilka Lindner, Petra Uta, and Torsten Beier for excellent technical assistance; Jacek Biernat for generating Tau proteins; and Walter Steffen for the anti-dynein antibody.

REFERENCES

1. Cleveland, D. W., Hwo, S. Y., and Kirschner, M. W. (1977) Physical and chemical properties of purified Tau factor and the role of Tau in microtubule assembly. *J. Mol. Biol.* **116,** 227–247

2. Drubin, D. G., and Kirschner, M. W. (1986) Tau protein function in living cells. *J. Cell Biol.* **103,** 2739–2746
3. Stamer, K., Vogel, R., Thies, E., Mandelkow, E., and Mandelkow, E. M. (2002) Tau blocks traffic of organelles, neurofilaments, and APP vesicles in neurons and enhances oxidative stress. *J. Cell Biol.* **156,** 1051–1063
4. Stoothoff, W., Jones, P. B., Spires-Jones, T. L., Joyner, D., Chhabra, E., Bercury, K., Fan, Z., Xie, H., Bacskai, B., Edd, J., Irimia, D., and Hyman, B. T. (2009) Differential effect of three-repeat and four-repeat Tau on mitochondrial axonal transport. *J. Neurochem.* **111,** 417–427
5. Seitz, A., Kojima, H., Oiwa, K., Mandelkow, E. M., Song, Y. H., and Mandelkow, E. (2002) Single-molecule investigation of the interference between kinesin, Tau and MAP2c. *EMBO J.* **21,** 4896–4905
6. Dixit, R., Ross, J. L., Goldman, Y. E., and Holzbaur, E. L. (2008) Differential regulation of dynein and kinesin motor proteins by Tau. *Science* **319,** 1086–1089
7. Vershinin, M., Carter, B. C., Razafsky, D. S., King, S. J., and Gross, S. P. (2007) Multiple-motor based transport and its regulation by Tau. *Proc. Natl. Acad. Sci. U.S.A.* **104,** 87–92
8. Wang, L., and Brown, A. (2002) Rapid movement of microtubules in axons. *Curr. Biol.* **12,** 1496–1501
9. Baas, P. W., Vidya Nadar, C., and Myers, K. A. (2006) Axonal transport of microtubules: the long and short of it. *Traffic* **7,** 490–498
10. Konzack, S., Thies, E., Marx, A., Mandelkow, E. M., and Mandelkow, E. (2007) Swimming against the tide: mobility of the microtubule-associated protein Tau in neurons. *J. Neurosci.* **27,** 9916–9927
11. Utton, M. A., Noble, W. J., Hill, J. E., Anderton, B. H., and Hanger, D. P. (2005) Molecular motors implicated in the axonal transport of Tau and α-synuclein. *J. Cell Sci.* **118,** 4645–4654
12. Cuchillo-Ibanez, I., Seereeram, A., Byers, H. L., Leung, K. Y., Ward, M. A., Anderton, B. H., and Hanger, D. P. (2008) Phosphorylation of Tau regulates its axonal transport by controlling its binding to kinesin. *FASEB J.* **22,** 3186–3195
13. Samsonov, A., Yu, J. Z., Rasenick, M., and Popov, S. V. (2004) Tau interaction with microtubules *in vivo*. *J. Cell Sci.* **117,** 6129–6141
14. Mercken, M., Fischer, I., Kosik, K. S., and Nixon, R. A. (1995) Three distinct axonal transport rates for Tau, tubulin, and other microtubule-associated proteins: evidence for dynamic interactions of Tau with microtubules *in vivo*. *J. Neurosci.* **15,** 8259–8267
15. Bormuth, V., Varga, V., Howard, J., and Schäffer, E. (2009) Protein friction limits diffusive and directed movements of kinesin motors on microtubules. *Science* **325,** 870–873
16. Furuta, K., Edamatsu, M., Maeda, Y., and Toyoshima, Y. Y. (2008) Diffusion and directed movement: *in vitro* motile properties of fission yeast kinesin-14 Pkl1. *J. Biol. Chem.* **283,** 36465–36473
17. Kapitein, L. C., Kwok, B. H., Weinger, J. S., Schmidt, C. F., Kapoor, T. M., and Peterman, E. J. (2008) Microtubule cross-linking triggers the directional motility of kinesin-5. *J. Cell Biol.* **182,** 421–428
18. Kim, Y., Heuser, J. E., Waterman, C. M., and Cleveland, D. W. (2008) CENP-E combines a slow, processive motor and a flexible coiled coil to produce an essential motile kinetochore tether. *J. Cell Biol.* **181,** 411–419
19. Lu, H., Ali, M. Y., Bookwalter, C. S., Warshaw, D. M., and Trybus, K. M. (2009) Diffusive movement of processive kinesin-1 on microtubules. *Traffic* **10,** 1429–1438
20. Okada, Y., and Hirokawa, N. (2000) Mechanism of the single-headed processivity: diffusional anchoring between the K-loop of kinesin and the C terminus of tubulin. *Proc. Natl. Acad. Sci. U.S.A.* **97,** 640–645
21. Reck-Peterson, S. L., Yildiz, A., Carter, A. P., Gennerich, A., Zhang, N., and Vale, R. D. (2006) Single-molecule analysis of dynein processivity and stepping behavior. *Cell* **126,** 335–348
22. Wang, Z., and Sheetz, M. P. (1999) One-dimensional diffusion on microtubules of particles coated with cytoplasmic dynein and immunoglobulins. *Cell Struct. Funct.* **24,** 373–383
23. Ali, M. Y., Krementsova, E. B., Kennedy, G. G., Mahaffy, R., Pollard, T. D., Trybus, K. M., and Warshaw, D. M. (2007) Myosin Va maneuvers through actin intersections and diffuses along microtubules. *Proc. Natl. Acad. Sci. U.S.A.* **104,** 4332–4336
24. Minoura, I., Katayama, E., Sekimoto, K., and Muto, E. (2010) One-dimensional Brownian motion of charged nanoparticles along microtubules: a model system for weak binding interactions. *Biophys. J.* **98,** 1589–1597
25. Ramey, V. H., Wang, H. W., Nakajima, Y., Wong, A., Liu, J., Drubin, D., Barnes, G., and Nogales, E. (2011) The Dam1 ring binds to the E-hook of tubulin and diffuses along the microtubule. *Mol. Biol. Cell* **22,** 457–466
26. Cooper, J. R., and Wordeman, L. (2009) The diffusive interaction of microtubule binding proteins. *Curr. Opin. Cell Biol.* **21,** 68–73
27. Helenius, J., Brouhard, G., Kalaidzidis, Y., Diez, S., and Howard, J. (2006) The depolymerizing kinesin MCAK uses lattice diffusion to rapidly target microtubule ends. *Nature* **441,** 115–119
28. Gustke, N., Trinczek, B., Biernat, J., Mandelkow, E. M., and Mandelkow, E. (1994) Domains of Tau protein and interactions with microtubules. *Biochemistry* **33,** 9511–9522
29. Scholz, T., Vicary, J. A., Jeppesen, G. M., Ulcinas, A., Hörber, J. K., and Antognozzi, M. (2011) Processive behaviour of kinesin observed using micro-fabricated cantilevers. *Nanotechnology* **22,** 095707
30. Rump, A., Scholz, T., Thiel, C., Hartmann, F. K., Uta, P., Hinrichs, M. H., Taft, M. H., and Tsiavaliaris, G. (2011) Myosin-1C associates with microtubules and stabilizes the mitotic spindle during cell division. *J. Cell Sci.* **124,** 2521–2528
31. Sbalzarini, I. F., and Koumoutsakos, P. (2005) Feature point tracking and trajectory analysis for video imaging in cell biology. *J. Struct. Biol.* **151,** 182–195
32. Zimmermann, D., Abdel Motaal, B., Voith von Voithenberg, L., Schliwa, M., and Ökten, Z. (2011) Diffusion of myosin V on microtubules: a fine-tuned interaction for which e-hooks are dispensable. *PLoS ONE* **6,** e25473
33. Burton, R. F. (1983) The composition of animal cells: solutes contributing to osmotic pressure and charge balance. *Comp. Biochem. Physiol. B* **76,** 663–671
34. Thorn, K. S., Ubersax, J. A., and Vale, R. D. (2000) Engineering the processive run length of the kinesin motor. *J. Cell Biol.* **151,** 1093–1100
35. Steffen, W., Hodgkinson, J. L., and Wiche, G. (1996) Immunogold localisation of the intermediate chain within the protein complex of cytoplasmic dynein. *J. Struct. Biol.* **117,** 227–235
36. Gestaut, D. R., Graczyk, B., Cooper, J., Widlund, P. O., Zelter, A., Wordeman, L., Asbury, C. L., and Davis, T. N. (2008) Phosphoregulation and depolymerization-driven movement of the Dam1 complex do not require ring formation. *Nat. Cell Biol.* **10,** 407–414
37. Powers, A. F., Franck, A. D., GesTaut, D. R., Cooper, J., Gracyzk, B., Wei, R. R., Wordeman, L., Davis, T. N., and Asbury, C. L. (2009) The Ndc80 kinetochore complex forms load-bearing attachments to dynamic microtubule tips via biased diffusion. *Cell* **136,** 865–875
38. Weinger, J. S., Qiu, M., Yang, G., and Kapoor, T. M. (2011) A nonmotor microtubule binding site in kinesin-5 is required for filament cross-linking and sliding. *Curr. Biol.* **21,** 154–160
39. Mukrasch, M. D., Biernat, J., von Bergen, M., Griesinger, C., Mandelkow, E., and Zweckstetter, M. (2005) Sites of Tau important for aggregation populate β-structure and bind to microtubules and polyanions. *J. Biol. Chem.* **280,** 24978–24986
40. Mukrasch, M. D., Bibow, S., Korukottu, J., Jeganathan, S., Biernat, J., Griesinger, C., Mandelkow, E., and Zweckstetter, M. (2009) Structural polymorphism of 441-residue Tau at single residue resolution. *PLoS Biol.* **7,** e34
41. Jeganathan, S., von Bergen, M., Brutlach, H., Steinhoff, H. J., and Mandelkow, E. (2006) Global hairpin folding of Tau in solution. *Biochemistry* **45,** 2283–2293
42. Jeganathan, S., von Bergen, M., Mandelkow, E. M., and Mandelkow, E. (2008) The natively unfolded character of Tau and its aggregation to Alzheimer-like paired helical filaments. *Biochemistry* **47,** 10526–10539
43. Kar, S., Fan, J., Smith, M. J., Goedert, M., and Amos, L. A. (2003) Repeat motifs of Tau bind to the insides of microtubules in the absence of Taxol. *EMBO J.* **22,** 70–77
44. Makrides, V., Massie, M. R., Feinstein, S. C., and Lew, J. (2004) Evidence for two distinct binding sites for Tau on microtubules. *Proc. Natl. Acad. Sci. U.S.A.* **101,** 6746–6751
45. Butner, K. A., and Kirschner, M. W. (1991) Tau protein binds to microtubules through a flexible array of distributed weak sites. *J. Cell Biol.* **115,** 717–730

46. Goode, B. L., Denis, P. E., Panda, D., Radeke, M. J., Miller, H. P., Wilson, L., and Feinstein, S. C. (1997) Functional interactions between the proline-rich and repeat regions of Tau enhance microtubule binding and assembly. *Mol. Biol. Cell* **8,** 353–365
47. Schaap, I. A., de Pablo, P. J., and Schmidt, C. F. (2004) Resolving the molecular structure of microtubules under physiological conditions with scanning force microscopy. *Eur. Biophys. J.* **33,** 462–467
48. Nakata, T., Sato-Yoshitake, R., Okada, Y., Noda, Y., and Hirokawa, N. (1993) Thermal drift is enough to drive a single microtubule along its axis even in the absence of motor proteins. *Biophys. J.* **65,** 2504–2510
49. Motegi, F., Zonies, S., Hao, Y., Cuenca, A. A., Griffin, E., and Seydoux, G. (2011) Microtubules induce self-organization of polarized PAR domains in *Caenorhabditis elegans* zygotes. *Nat. Cell Biol.* **13,** 1361–1367
50. Howard, J., Grill, S. W., and Bois, J. S. (2011) Turing's next steps: the mechanochemical basis of morphogenesis. *Nat. Rev. Mol. Cell Biol.* **12,** 392–398
51. Li, X., Kumar, Y., Zempel, H., Mandelkow, E. M., Biernat, J., and Mandelkow, E. (2011) Novel diffusion barrier for axonal retention of Tau in neurons and its failure in neurodegeneration. *EMBO J.* **30,** 4825–4837
52. Nakata, T., Niwa, S., Okada, Y., Perez, F., and Hirokawa, N. (2011) Preferential binding of a kinesin-1 motor to GTP-tubulin-rich microtubules underlies polarized vesicle transport. *J. Cell Biol.* **194,** 245–255
53. McVicker, D. P., Chrin, L. R., and Berger, C. L. (2011) The nucleotide-binding state of microtubules modulates kinesin processivity and the ability of Tau to inhibit kinesin-mediated transport. *J. Biol. Chem.* **286,** 42873–42880
54. Konishi, Y., and Setou, M. (2009) Tubulin tyrosination navigates the kinesin-1 motor domain to axons. *Nat. Neurosci.* **12,** 559–567